ORIGINAL PAPER

Corrosion inhibition and adsorption behavior of imidazoline salt on N80 carbon steel in CO_2-saturated solutions and its synergism with thiourea

P. C. Okafor · C. B. Liu · X. Liu · Y. G. Zheng · F. Wang · C. Y. Liu · F. Wang

Abstract The inhibition and adsorption behavior of 2-undecyl-1-sodium ethanoate-imidazoline salt (2M2) and thiourea (TU) on N80 mild steel in CO_2-saturated 3 wt.% NaCl solutions was studied at 25°C, pH 4, and 1 bar CO_2 partial pressure using electrochemical methods. It was found that inhibition efficiency ($\eta\%$) increased with increase in 2M2 concentration but decreased with increase in TU concentration with optimum $\eta\%$ value at 20 mg l^{-1} TU. The data suggest that the compounds functioned via a mixed-inhibitor mechanism. The inhibition process is attributed to the formation of an adsorbed film of 2M2 and TU via the inhibitors polycentric adsorption sites on the metal surface which protects the metal against corrosion. A synergistic effect was observed between TU and 2M2. Potential of unpolarizability, E_u, was observed in the presence of 100 mg l^{-1} TU which was shifted positively in the presence of 2M2–100 mg l^{-1} TU blends, which suggests that the presence of 2M2 stabilized the adsorption of TU molecules on the surface of the metal. The adsorption characteristics of 2M2 were approximated by Langmuir adsorption isotherm.

Introduction

Corrosion of metal in CO_2-saturated solutions is a complex process due to the variety of corrosion active species present in the solution and has been widely investigated [1–7] and recognized as a major factor in the degradation of oil and gas pipelines. To reduce the aggressiveness of CO_2-saturated solutions, inhibitors are used and acknowledged to be the most cost-effective and flexible means of corrosion control in the oil and gas production industry [8–11]. One class of inhibitor which has proven to be most effective in CO_2-saturated systems and widely applied for protecting CO_2 corrosion of oil and gas pipelines is the imidazolines [10–17]. This is probably due to their effectiveness, availability, and environmental friendliness. In order to further improve the performance of imidazolines as inhibitor of CO_2 corrosion, commercial inhibitor formulations usually consist of its mixtures with other compounds [18].

One organic compound which is a component of some commercial inhibitor formulations for acid media is thiourea (TU). The use of TU as corrosion inhibitor of metals in acid media goes as far back as 1946 [19] and has attracted lots of researchers into investigating its effects and mechanism on the corrosion of metals, owing to its strong adsorbability and its consequent influence on the interfacial characteristics [20–26]. TU is reported to have a narrow inhibition

P. C. Okafor · C. B. Liu · X. Liu · Y. G. Zheng (✉)
State Key Laboratory for Corrosion and Protection,
Institute of Metal Research, CAS,
62 Wencui Road,
Shenyang 110016, Liaoning Province, People's Republic of China
e-mail: ygzheng@imr.ac.cn
e-mail: icpmkaist@yahoo.com

P. C. Okafor
Department of Pure and Applied Chemistry,
University of Calabar,
P. M. B.,
1115 Calabar, Nigeria
e-mail: pcokafor@gmail.com

F. Wang · C. Y. Liu · F. Wang
Jilin Oilfield Corporation of PetroChina,
Songyuan 138000, Jilin Province, People's Republic of China

concentration range in acid media, beyond which it turns into a corrosion accelerator [20–22]. This concentration range is reported to be temperature and pH dependent [21, 22]. Until recently [27], the use of TU as corrosion inhibitor in CO₂-saturated solutions has not been published in the open literatures even though commercial formulations are composed of it. This is probably due to the variety of the complex dynamic phenomena surrounding TU chemistry [28] which makes its inhibition mechanism very poorly understood, especially in complex CO₂-saturated systems.

It is an established fact that the inhibiting action of organic molecules is due to the adsorption of the additive on the metal/solution interface which may lead to a structural modification in the electric double layer with subsequent reduction in the rates of the anodic as well as the cathodic electrochemical reactions, and that the molecular structure, and more especially the functional group of the inhibiting molecules has a large influence on corrosion inhibition mechanism [29]. This adsorption phenomenon could occur via electrostatic attraction between the charged metal and the charged inhibitor molecules, dipole-type interaction between unshared electron pairs in the inhibitor with the metal, pi-interaction with the metal, and a combination of all of the above processes [29–31]. However, the mutual effects of two different organic compounds having two different functional groups, which may influence the adsorption characteristics and consequently the corrosion mechanism has not been properly documented.

In continuation of an extensive project being carried out in our laboratories on the inhibitive properties of imidazoline derivatives in CO₂-saturated NaCl solutions under various experimental conditions, we present here the adsorption and inhibition mechanism of an imidazoline salt, 2-undecyl-1-sodium ethanoate-imidazoline salt (2M2) containing both >C=O and >N– functional groups (Fig. 1a), and its synergistic behavior with thiourea, a thiocarbonyl compound containing >N– and >C=S functional groups (Fig. 1b), on N80 mild steel in CO₂-saturated 3% NaCl solutions using electrochemical techniques. The techniques are well suited for in situ monitoring of electrochemical processes in the metal/solution interface from which the adsorption as well as corrosion inhibition mechanism can be deduced. The surface morphological changes on the corroding steel surface were observed using scanning electron microscope (SEM).

Experimental

Materials preparation

N80 carbon steel cut from its parent pipe was used as the test material for these experiments and has the chemical
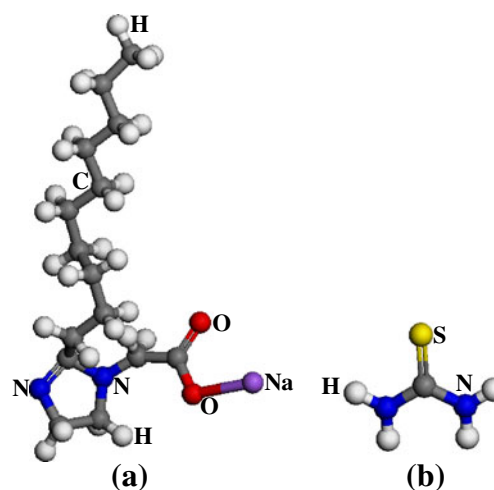

Fig. 1 Three-dimensional structure of **a** 2-undecyl-1-sodium ethanoate-imidazoline salt (2M2) and **b** thiourea

composition shown in Table 1. The steel sheet was cut into coupons of dimension 1×1×0.8 cm. The coupons were degreased with acetone in an ultrasonic water bath for about 10 min, air dried, embedded in two-component epoxy resin, and mounted in a PVC holder. A copper wire was soldered to the rear side of the coupon as an electrical connection. The exposed surface of the electrode (of area 1 cm²) was wet polished with silicon carbide abrasive paper up to 800 grits, rinsed with ethanol, placed in an ultrasonic acetone bath for about 5 min to remove possible residue of polishing and air dried. This was used as the working electrode during the electrochemical test.

The test media was 3 wt.% NaCl solution saturated with carbon dioxide gas at atmospheric pressure by continuous purging with carbon dioxide. The gas exit was sealed with distilled water. When needed, sodium bicarbonate (NaHCO₃), was added to adjust the pH. The temperature was maintained at 25±1°C in all the experiments by placing the cell on a thermostated water bath. The pH was monitored with PB-10 Sartorius pH/temperature (°C) meter (with accuracy of ±0.01) that was carefully calibrated with two buffer solution (pH 4 and 7). Electrochemical measurements were made using a PARSTAT® 2273 electrochemical measurement system connected to a computer. All chemicals used were of analar grade.

Experimental procedure

Experiments were conducted in a three-electrode 1,000-ml glass cell setup with the counter electrode made of a platinum foil and the reference electrode being a saturated calomel electrode (SCE) connected to the cell externally through a Luggin capillary tube positioned close to the working electrode (N80 carbon steel) by 3 mm apart to minimize the ohmic potential drop.

Table 1 Chemical composition of the N80 carbon steel

Element	C	Si	Mn	P	S	Al	Cu	Nb	Ni
Composition (wt.%)	0.52	0.23	1.50	0.011	0.008	0.01	0.07	<0.005	0.02

The glass cell was filled with 750 ml of the test solution, de-aerated and saturated with carbon dioxide. The free corrosion potential was followed immediately after immersion until the potential stabilized within ±1 mV. Linear polarization resistance (LPR) measurements were taken at ±5 mV around the corrosion potential, by using a potentiodynamic scan at 0.1 mV s^{-1} followed by EIS measurements over the frequency range of 100 kHz to 10 mHz with a signal amplitude perturbation of 5 mV. The potentiodynamic polarization sweeps were conducted at a sweep rate of 0.2 mV s^{-1}. The solution and metal coupon were changed after each sweeps. All experiments were conducted at pH 4 to ascertain a uniform concentration of the corrosive carbonic species. For each experimental condition, two to three measurements were performed to estimate the repeatability. The repeatability was quite good, and the changes observed in the results reflect influences of various parameters beyond the experimental error.

Results and discussion

Inhibition by imidazoline (2M2)

Electrochemical impedance measurements

The impedance plot for N80 carbon steel in 3% NaCl solutions in the absence and presence of 2M2 at pH 4 and 25°C is illustrated as Nyquist plots in Fig. 2. All the EIS plots have a depressed semicircle at high frequencies with center under the real axis, which is the characteristic for solid electrodes and has been attributed to roughness and other inhomogeneties of the electrode [32, 33]. The high-frequency capacitive loop is attributed to the double layer capacity in parallel with the charge-transfer resistance (R_{ct}). Though it is probably a composite value representing dissolution of the iron and other alloying elements, it is governed by the dissolution of iron since iron is the major component of the alloy and iron is a highly active metal in acidic media [34].

In the absence of the inhibitor (Fig. 2 inset), the impedance spectrum is characterized by a low-frequency inductive loop. The inductive loop is ascribed to the adsorption of species exhibiting negative change in the surface coverage with potential [34, 35] on the surface of the metal. As the 2M2 is added into the system, the inductive loop is transformed into an oblique line (of about 45°) at the low frequency; a typical feature of Warburg

impedance. The Warburg impedance is an indication of diffusion control as species transfer through surface film or mass transport through the electrolyte. A closer look at the curves also shows an indication of a capacitive loop at low frequency in the presence of 2M2.

Two apparent characteristics are observed on the impedance spectra in Fig. 2 on addition of 2M2. Firstly, the high-frequency capacitive loop increases with increase in 2M2 concentration. The appreciation of the impedance can be ascribed to the inhibition of the iron dissolution process due to the adsorption of 2M2 molecules on the iron surface. Secondly, the low-frequency capacitive loop/ Warburg impedance increases in length with increase in 2M2 concentration. This is assumed to be due to another factor that affects the corrosion process. This factor is also dependent on the 2M2 concentration.

The impedance data were analyzed using the equivalent circuit (EC) models shown in Fig. 3. The circuit comprises of a hierarchical arrangement consisting of two stacked resistance-constant phase element pairs. R_s represents the solution resistance, Q_1 and Q_2 represent the constant phase element (CPE), R_{ct} the charge-transfer resistance, and R_a the equivalent resistance. In the absence of inhibitor (blank), a negative resistance and capacitance CPE were used to represent the arcs with an inductive character, since it is more difficult from a physical view point to justify the use of very high inductance. This is in accordance with Macdonald's approach [34, 36]. Warburg impedance (W) was incorporated within the equivalent circuit (Fig. 3b) to model the low frequency response observed in the presence of the inhibitor.

In order to account for the roughness and inhomogeneities of the solid electrode [37–39] and the frequency
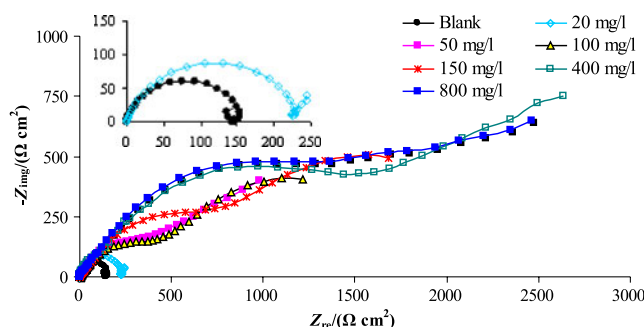

Fig. 2 Nyquist plots for N80 carbon steel in CO$_2$-saturated 3% NaCl solutions containing 2M2 at pH 4 and 25°C. *Inset* Blank and 20 mg l^{-1} 2M2

independent phase shift between an applied AC potential and its current response [40], the capacitance in the ECs is substituted by an empirical constant phase element. The CPE has been extensively described in the literature [41–43]. The impedance, Z, of the CPE is defined as:

$$Z_{CPE} = Y_o^{-1}(j\omega)^{-n} \tag{1}$$

where Y_o and n are the CPE constant and exponent respectively, ω is the angular frequency in rad s^{-1} ($\omega = 2\pi f$) and $j^2 = -1$ an imaginary number. The characteristic frequencies f_{max} were obtained from the semicircles maxima and used to calculate the associated capacitance (C) from the equation [44]:

$$C = Y_o(2\pi f_{max})^{n-1} \tag{2}$$

The fitting Nyquist plots deduced from the experimental and simulated data, shown in Fig. 4, show that the fitting results are in good agreements with the experimental data.

In accordance with the EC given in Fig. 3b, the polarization resistance (R_p) is given as:

$$R_p = R_{ct} + R_a \tag{3}$$

where R_a is the equivalent resistance. The R_p derived from the Nyquist plots are given in Table 2. The values were found to increase with increase in 2M2 concentration indicating inhibition of the corrosion process. The R_p values measured from the LPR technique, also shown in Table 2 are in good agreement with the determined R_p values from the impedance plots.
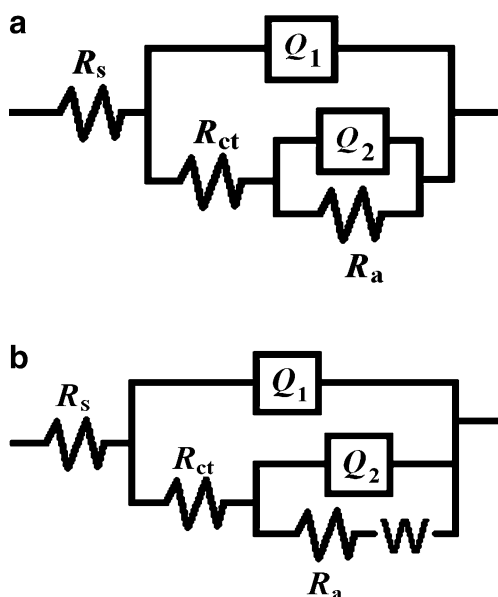

Fig. 3 The electrochemical equivalent circuit used for simulation of impedance data of N80 mild steel electrodes in **a** uninhibited and **b** inhibited CO$_2$-saturated 3% NaCl solutions
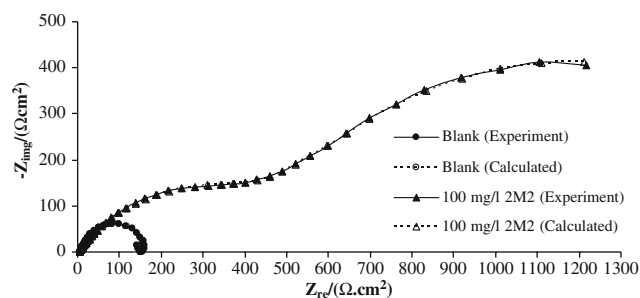
Fig. 4 Simulated and experimentally generated impedance diagrams for N80 mild steel in CO$_2$-saturated 3% NaCl solutions in the absence (blank) and presence of 100 mg l^{-1} 2M2 at pH 4 and 25 °C

From the polarization resistance values, the inhibition efficiency ($\eta\%$) values were determined from the equation:

$$\eta\% = \frac{R_{p(inh)} - R_p}{R_{p(inh)}} \times 100 \tag{4}$$

where R_p and $R_{p(inh)}$ are the uninhibited and inhibited polarization resistance, respectively. The inhibition efficiency was found to increase with increase in 2M2 concentration and the maximum inhibition efficiency (of about 94.2%) was obtained at 400 mg l^{-1} 2M2. The inhibition efficiency values obtained for the EIS and LPR methods are in good agreement.

Potentiodynamic polarization measurements

Figure 5 shows the potentiodynamic polarization curves of N80 mild steel electrodes in CO$_2$-saturated 3% NaCl solutions containing different concentrations of 2M2. The corresponding corrosion potential (E_{corr}) and corrosion current density (i_{corr}) are listed in Table 2. With the increase of 2M2 concentration, both the anodic and cathodic currents were inhibited. Based on this result, 2M2 is considered as a mixed-type inhibitor. Meaning that it reduces the anodic dissolution of the mild steel and also retards the cathodic reactions. Concerning the anodic region in relation to the zero current density potential, there is no evidence of passive film formation onto the electrode surface either in the presence or in the absence of the inhibitor. However, an anodic displacement of the corrosion potential (E_{corr}) and a decrease in the corrosion current density (i_{corr}) with increase in 2M2 concentration were also observed. This indicates the inhibiting effect of 2M2 on the mild steel corrosion which can be related to its adsorption on the steel surface blocking active sites.

A closer observation of the polarization curves in Fig. 5 reveals two linear portions on the anodic polarization curves at 2M2 concentration ≥50 mg l^{-1}. This behavior indicated that the anodic reaction in the presence of 2M2

Table 2 Polarization, EIS, and LPR parameters for N80 mild steel in CO_2-saturated 3% NaCl solutions in the absence and presence of 2M2 at 25 °C

2M2 concentration (mgl^{-1})	Polarization method			EIS method		LPR method	
	$-E_{corr}$ (V_{SCE})	i_{corr} (μAcm^{-2})	$\eta\%$	R_p (Ωcm^2)	$\eta\%$	R_p (Ωcm^2)	$\eta\%$
Blank	712.3	53.0	–	153.5	–	169.8	–
20	713.6	32.7	38.3	226.3	32.2	291.7	41.8
50	697.5	14.5	72.7	975.5	84.3	1,036.0	83.6
100	639.2	5.4	89.9	1,212.3	87.3	1,493.0	88.6
150	639.2	4.5	91.5	1,680.9	90.9	2,373.0	92.8
400	665.1	3.3	93.8	2,637.2	94.2	2,827.0	94.0
800	619.2	3.9	92.5	2,463.5	93.8	2,504.0	93.2

exhibits different characteristics at different potentials. At low potentials, the dissolution rate is dependent on the concentration of adsorbed 2M2 molecules. Increase in the potentials leads to desorption of the adsorbed 2M2 molecules. At a given potential, which is dependent on the concentration of 2M2 molecules, the dissolution rate is under control by the same species determining the reaction rate in the absence of inhibitor (blank). This observation is clearly seen and discussed more in the presence of inhibitor blends (2M2–TU).

From the calculated values of i_{corr}, the inhibition efficiency ($\eta\%$) of 2M2 was calculated from the following equation:

$$\eta\% = \frac{i_{corr}^o - i_{corr}}{i_{corr}^o} \times 100 \tag{5}$$

where i_{corr}^o and i_{corr} are the uninhibited and inhibited corrosion current densities, respectively. The results obtained are as shown in Table 2. It can be seen that 2M2 inhibits the corrosion of N80 carbon steel to an appreciable extent and that the extent of inhibition is dependent on the inhibitor concentration. This is consistent with the EIS and LPR results.
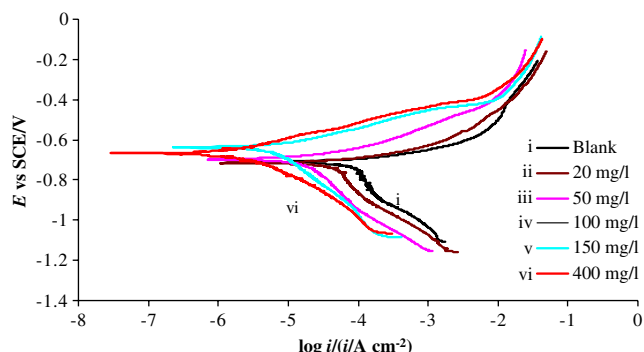
Adsorption behavior

Figure 6 shows the adsorption curve for 2M2 on N80 mild steel in CO_2-saturated 3% NaCl solutions at 25 °C. The plot is characterized by an initial steeply rising part indicating the formation of a monolayer adsorbate film on the mild steel surface [45, 46] and as more inhibitor molecules become adsorbed at higher concentration, the adsorption rate is reduced. From a theoretical standpoint, the inhibition action of organic molecules has been regarded as a simple substitution process, in which an inhibitor molecule (I) in the aqueous phase substitutes an x number of water molecules adsorbed on the surface [31, 47, 48]:

$$I_{(aq)} + xH_2O_{(ads)} \rightleftarrows I_{(ads)} + xH_2O_{(aq)} \tag{6}$$
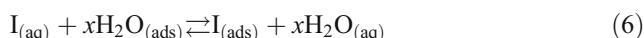
The inhibitor molecules may then combine with Fe^{2+} ions on the metal surface, forming metal–inhibitor complex. The resulting complex could, depending on its relative solubility, either inhibit or catalyze further metal dissolution [45].

Based on the electrochemical data in this project, the possible processes involved in the inhibition process on the electrode surface are, the dissolution of iron Eq. 7,
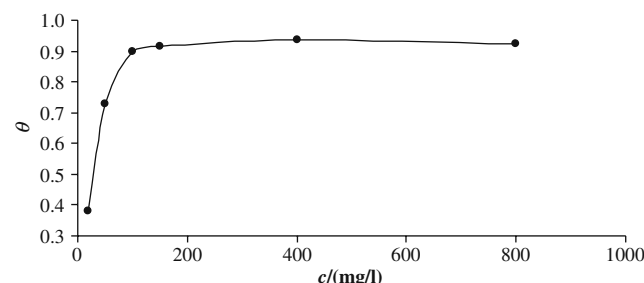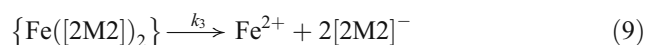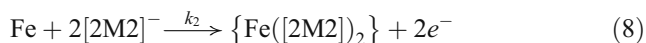
Fig. 5 Polarization curves for N80 carbon steel in CO_2-saturated 3% NaCl solutions containing 2M2 at pH 4 and 25 °C

Fig. 6 Adsorption curve for 2M2 on N80 mild steel in CO_2-saturated 3% NaCl solutions at pH 4 and 25 °C

the formation of an insoluble iron–imidazoline (Fe([2M2])$_2$) complex (the inhibiting film) Eq. 8 and the dissociation of Fe([2M2])$_2$ complex Eq. 9:

$$Fe \xrightarrow{k_1} Fe^{2+} + 2e^- \qquad (7)$$

$$Fe + 2[2M2]^- \xrightarrow{k_2} \left\{Fe([2M2])_2\right\} + 2e^- \qquad (8)$$

$$\left\{Fe([2M2])_2\right\} \xrightarrow{k_3} Fe^{2+} + 2[2M2]^- \qquad (9)$$

Equation 8 is assumed irreversible and the dissociation of the iron–imidazoline complex Eq. 9 negligible. Such complexation process is combined with adsorption of the inhibitor [24]. Inspection of the imidazoline structures in Fig. 1 reveals that 2M2 is composed of a five-member ring containing nitrogen elements, a C-11 saturated hydrophobic group and a hydrophilic ethanoate ion. A compound with polycentric adsorption sites of this nature may interact with the corroding metal and hence inhibit the corrosion reaction in one or a combination of ways. Thus, it may be difficult to assign a single general inhibition mechanism to the retardation of the corrosion process. However, in addition to the insoluble Fe–2M2 complex found, 2M2 can also be adsorbed on the metal surface by the formation of an iron–nitrogen coordination bond and by a pi-electron interaction between the pi-electron in the head group and the iron. This adsorption gives rise to a large covered surface area with a small number of adsorbed molecules. Therefore, high inhibition efficiency could be obtained by relatively low concentrations of the imidazoline. The adsorption on the surface of the mild steel creates a barrier for mass and charge transfer. At the same time, the increase of inhibitor concentration above a certain value has little effect on the inhibition efficiency. This conclusion is confirmed by the fact that the inhibition efficiency does not increase linearly with 2M2 concentration, as shown in Fig. 6. As revealed from the figure, the inhibition efficiency maintained almost constant values for 2M2 concentrations above 100 mg l^{-1}.

It is acknowledged that adsorption isotherms provide useful insights into the characteristics of the adsorption process and the mechanism of corrosion inhibition [49]. The experimental data obtained from the potentiodynamic polarization measurements were applied to different adsorption isotherm equations. It was found that the data fitted the Langmuir adsorption isotherm (Fig. 7). According to the Langmuir adsorption isotherm, there are no interaction forces existing between the adsorbed molecules, and the energy of adsorption is independent of the surface
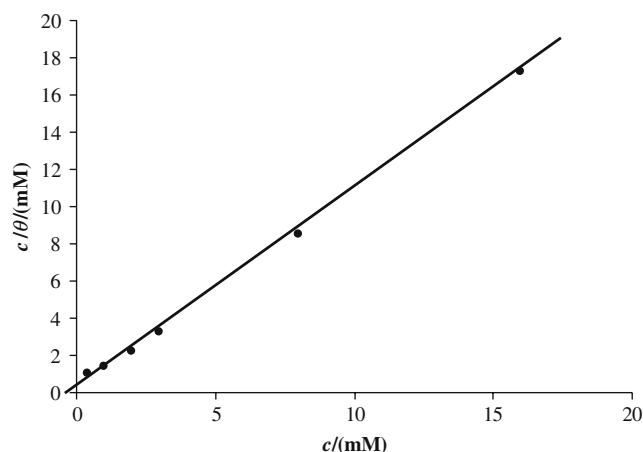

Fig. 7 Langmuir isotherm for the adsorption of 2M2 on the surface of N80 mild steel in CO$_2$-saturated 3% NaCl solutions at pH 4 and 25 °C

coverage (θ). The Langmuir adsorption isotherm could be represented using the equation [50]:

$$c/\theta = 1/k_{ads} + c \qquad (10)$$

where θ is the degree of surface coverage ($\theta = \eta\%/100$), k_{ads} is the equilibrium (or binding) constant of the adsorption reaction and c is the inhibitor concentration (in moles/l). The k_{ad} value of 3,579.1 was deduced from the plot and denotes the strength between the adsorbate and adsorbent. Large values of k_{ad} imply more efficient adsorption. The constant k_{ad} is related to the standard free energy of adsorption ΔG^o_{ads} by the equation:

$$k_{ads} = \frac{1}{55.5} \exp\left(\frac{-\Delta G^o_{ads}}{RT}\right) \qquad (11)$$

The value of 55.5 being the concentration of water in solution expressed in moles per liter. The calculated ΔG^o_{ads} value of −30.23 KJ mol^{-1} indicates a spontaneous chemical adsorption of 2M2 on the surface of the metal at 25 °C.

Effects of thiourea

Thiourea has been widely used as corrosion inhibitor and interacts strongly with the surfaces of d-metals (e.g. iron). This interaction has the character of chemisorption and it is similar to those of halide ions that involves sharing or donation of electron pairs [51, 52]. It is however reported to progressively lose its efficiency at higher concentration due to formation of soluble thiourea complex [24, 53].

Figure 8 illustrates the impedance spectrum (as Nyquist plots) for N80 mild steel in CO$_2$-saturated 3% NaCl solutions containing different concentrations of TU (0–100 mg l^{-1}) at pH 4 and at 25 °C. All the spectra consisted
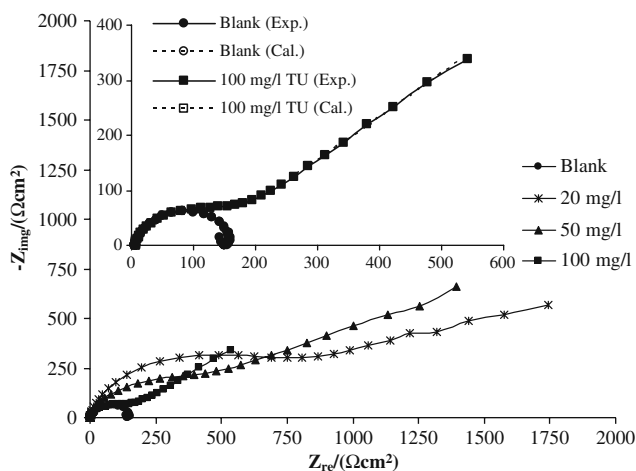
Fig. 8 Nyquist plots for N80 carbon steel in CO_2-saturated 3% NaCl solutions containing TU at pH 4 and 25°C

of single depressed semicircles similar to those obtained in the presence of 2M2. At the studied concentrations, the diameter semicircular arc decreases with the increase of thiourea concentration but greater than that obtained in the absence of inhibitor (blank). The decrease is attributed to the reduction of the inhibition process probably due to a possible formation of soluble thiourea complex.

The impedance data were analyzed using the equivalent circuit models shown in Fig. 3 and the fitting Nyquist plots deduced from the experimental and simulated data, shown in Fig. 8 (inset) indicate that the experimental and calculated results are in good agreements. The electrochemical parameters from both the electrochemical impedance and polarization measurements are listed in Table 3. The addition of thiourea increased the R_p values, indicating inhibition ability. The R_p values, however, decreased with increase in TU concentration. From the R_p values, the inhibition efficiency was deduced using Eq. 4. Inhibition efficiency was observed to decrease with increase in TU concentration. The optimum inhibition efficiency value was obtained at 20 mg l^{-1} TU. A similar trend and optimum TU concentration were previously reported by He et al. [27] for X70 steel in saline solution saturated with CO_2.

Figure 9 depicts the polarization curves for N80 mild steel in CO_2-saturated 3% NaCl solutions containing different concentrations of TU (0–100 mg l^{-1}) at pH 4 and at 25°C. The polarization parameters deduced from the curves are given in Table 3. TU was observed to significantly reduce the anodic and cathodic reactions as evident in the reduced corrosion current densities and E_{corr} was also observed to shift negatively with increase in TU concentration. These characteristics indicate that TU is a mixed corrosion inhibitor for N80 mild steel in CO_2-saturated 3% NaCl solutions under the present experimental conditions. At 100 mg l^{-1} TU there was an indication of a current "plateau" at the anodic curve resulting in two potentials; the corrosion potential E_{corr} and the potential of unpolarizability E_u. Similar behavior has been previously reported for the acidic dissolution of iron in the presence of iodide and organic inhibitors of different compositions [54–59]. E_u indicates the commencement of desorption of strongly adsorbed species on the electrode surface, above which the coverage of inhibitor decreases rapidly [54, 58]. The mechanism for such anodic dissolution of metals in the presence of inhibitors (in this case TU) that results in the presence of E_u is as explained in Okafor and Zheng [59].

Inspection of the structure of TU (Fig. 1b) reveals that the organic compound contains both N and S atoms. S-containing substances have been shown to preferentially chemisorb on the anodic sites on the surface of iron in acidic media, whereas N-containing substances tend to get protonated and preferentially physisorb on the cathodic sites [60, 61]. Thus, TU has the ability to inhibit both the anodic and cathodic reactions, giving rise to the observed mixed inhibition mechanism.

In order to access the mutual effects of TU and 2M2 on the corrosion of N80 mild steel in CO_2-saturated 3% NaCl solutions, electrochemical measurements were taken in solutions containing 100 mg l^{-1} TU–20 mg l^{-1} 2M2 and 100 mg l^{-1} TU–400 mg l^{-1} 2M2 corresponding to [TU]/[2M2] ratios of 5:1 and 1:4, respectively. These concentrations were chosen to access the interaction of TU and 2M2 at very low and very high 2M2 concentrations,

Table 3 Polarization, EIS, and LPR parameters for N80 mild steel in CO_2-saturated 3% NaCl solutions in the absence and presence of TU at 25°C

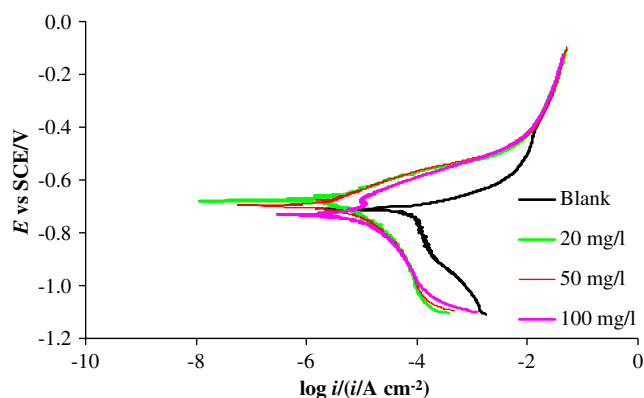| TU concentration (mgl^{-1})	Polarization method			EIS method		LPR method	
	$-E_{corr}$ (V$_{SCE}$)	i_{corr} (μAcm^{-2})	$\eta\%$	R_{ct} (Ωcm^2)	$\eta\%$	R_p (Ωcm^2)	$\eta\%$
Blank	712.3	53.0	–	153.5	–	169.8	–
20	679.8	4.0	92.5	1,745.8	91.2	2,038.0	91.7
50	696.6	7.6	85.8	1,392.7	89.0	1,734.0	90.2
100	730.3	14.0	73.6	535.9	71.4	769.7	77.9

Fig. 9 Polarization curves for N80 carbon steel in CO_2-saturated 3% NaCl solutions containing TU at pH 4 and 25 °C

respectively. Based on the least inhibition efficiency obtained and the presence of E_u at 100 mg l^{-1} TU, the later was chosen for synergistic investigation with 2M2. The results obtained are as depicted in Fig. 10 and the electrochemical data listed in Table 4.
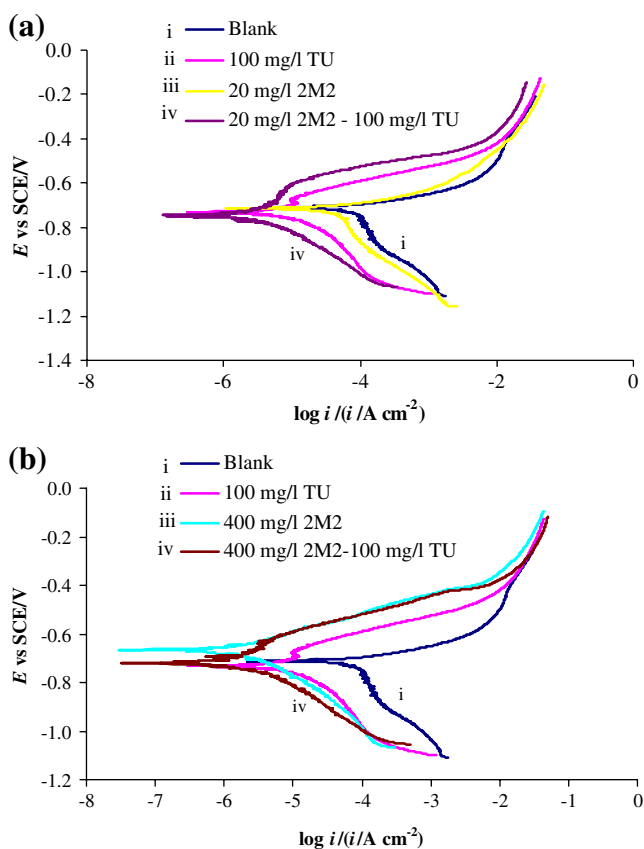

Fig. 10 Polarization curves for N80 carbon steel in CO_2-saturated 3% NaCl solutions in the absence and presence of **a** 20 mg l^{-1} 2M2, 100 mg l^{-1} TU, and 20–100 mg l^{-1} TU and **b** 400 mg l^{-1} 2M2, 100 mg l^{-1} TU and 400 mg l^{-1} 2M2–100 mg l^{-1} TU at pH 4 and 25 °C

From Fig. 10, it is observed that the TU–2M2 combinations produced more effects on the anodic and cathodic reactions compared to those displayed by only TU and 2M2, and slightly shifts E_{corr} in the cathodic direction compared to the blank solution. This indicates a synergistic effect between TU and 2M2. At low 2M2 concentrations (100 mg l^{-1} TU–20 mg l^{-1} 2M2) depicted in Fig. 10a, the addition of 20 mg l^{-1} 2M2 to 100 mg l^{-1} TU had a little effect on E_{corr} compared to the values of TU alone and also resulted in a positive shift of the potentials of unpolarizability, E_u. This is interpreted to be due to increasing stability of the species adsorbed on the electrode surface [58]. E_u was not observed in the presence of 2M2 but in 100 mg l^{-1} TU; therefore, the improved inhibition efficiency is most likely due to the improved adsorption stability of TU species by 2M2. At high 2M2 concentration (100 mg l^{-1} TU–400 mg l^{-1} 2M2) depicted in Fig. 10b, E_{corr} was not significantly affected compared to that of 100 mg l^{-1} TU and a positive shift in E_u was also observed. However, the rate of the anodic reaction beyond E_u was observed to be at the same rate as those in the presence of 400 mg l^{-1} 2M2 alone. This indicates that the blend inhibitors (TU–2M2) combines the advantages of both TU (high E_u) and 2M2 (high anodic inhibition). From the results obtained it could be deduced that the shifting of E_{corr} towards the negative in the blend inhibitors is due to the adsorption of TU and the increase in the values of E_u due to the increase in stability of TU adsorption by 2M2. The latter may be caused by the interaction between TU/(Fe–TU) complex and 2M2 ions. Chemisorption of TU molecules, like that of I^- as hinted by Kuznetsov and Andreev [62], may decrease the hydrophilicity of metal surfaces and enhance the adsorption of 2M2. Also, competitive adsorption between TU and 2M2 may also contribute to the observed synergism. However, from the results obtained in this study, the co-operative adsorption between TU and 2M2 seems to be the dominant mechanism of inhibition.

Surface morphological observation

The surface morphologies of the N80 carbon steel specimen in CO_2-saturated 3% NaCl solutions in the absence and presence of 20 mg l^{-1} 2M2, 100 mg l^{-1} TU, and 20 mg l^{-1} 2M2–100 mg l^{-1} TU at 25 °C and pH4 after 2 h of immersion were examined using SEM. The results obtained are as shown in Fig. 11. In the absence of inhibitors (Fig. 11a) a very rough surface was observed due to rapid corrosion attack on the carbon steel in the CO_2-saturated solution. The attack was relatively general with slight evidence of selective corrosion. In the presence of the 20 mg l^{-1} 2M2 (Fig. 11b) and 100 mg l^{-1} TU (Fig. 11c), the rough surface is reduced indicating the inhibition effect of 2M2 and TU on the surface of the metal. This, as described

Table 4 Polarization parameters for N80 mild steel in CO$_2$-saturated 3% NaCl solutions in the absence and presence of 2M2/TU mixture at 25°C

2M2/TU concentration (mgl^{-1})/mgl^{-1}	Ratio (2M2/TU)	Polarization method		
		$-E_{corr}$ (V$_{SCE}$)	i_{corr} (μAcm^{-2})	$\eta\%$
Blank	Blank	712.3	53.0	–
20/100	1/5	743.9	3.0	94.3
400/100	4/1	721.9	1.5	97.2

earlier, is due to the formation of protective inhibitor layers that create a barrier for mass and charge transfer. However, the selective dissolution of some areas on the surface of the metal is visible indicating that the inhibitor layers are not very protective and thus the anodic and cathodic sites on the surface of the metal are still exposed to the corrosion active species in the CO$_2$-saturated system. In the presence of the inhibitors blend, 20 mg l^{-1} 2M2–100 mg l^{-1} TU (Fig. 11d), the surface roughness is visibly reduced compared to those in the presence of 20 mg l^{-1} 2M2 and 100 mg l^{-1} TU. This behavior is related to the proposed synergistic effects between TU and 2M2 leading to a more compact and protective film on the surface of the metal, and an enhanced inhibition efficiency of over 94%.

Conclusions

The inhibition behavior of 2M2, TU, and TU–2M2 blends for N80 mild steel in CO$_2$-saturated 3% NaCl solutions was investigated and the following conclusions were drawn:

1. 2M2 and TU are effective inhibitors for the corrosion of N80 mild steel in CO$_2$-saturated 3% NaCl solutions and the extent of inhibition is dependent on the compounds concentration. The inhibition efficiency ($\eta\%$) increased with increase in 2M2 concentration but decreased with increase in TU concentration with optimum $\eta\%$ value at 20 mg l^{-1} TU. Both compounds functioned via a mixed-inhibitor mechanism.
2. The compounds inhibit the corrosion reactions via their polycentric adsorption sites on the surface of the metal. This adsorption gives rise to a large covered surface area with a small number of adsorbed molecules.
3. The adsorption characteristics of 2M2 were approximated by Langmuir adsorption isotherm.
4. A synergistic effect was observed between TU and 2M2 due to interaction between the inhibiting compounds. Potential of unpolarizability, E_u, was observed

Fig. 11 Scanning electron micrographs of the N80 mild steel surface after 2 h immersion in CO$_2$-saturated 3% NaCl solutions in the **a** absence and presence of **b** 20 mg l^{-1} 2M2, **c** 100 mg l^{-1} TU and **d** 20 mg l^{-1} 2M2–100 mg l^{-1} TU at 25°C and pH 4
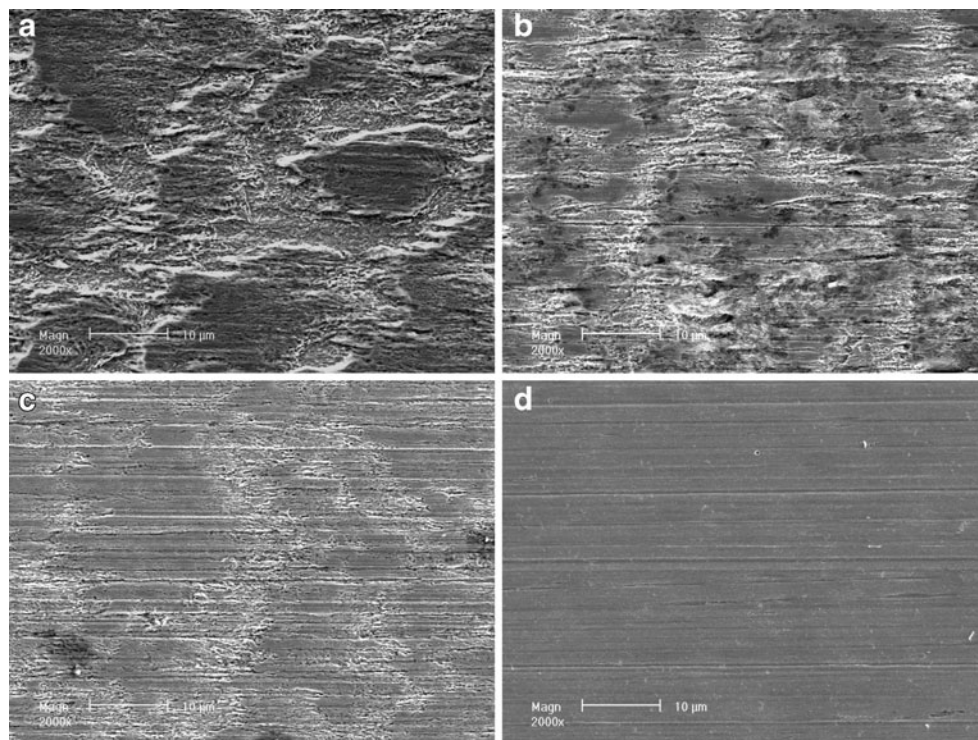
in the presence of 100 mg l^{-1} TU which was shifted positively in the presence of 2M2. The results suggest that the presence of 2M2 stabilized the adsorption of TU molecules on the surface of the metal.

References

1. Gray LGS, Anderson BG, Danysh MJ, Tremaine PR (1990) Proceedings of corrosion/1990, paper no 40. NACE International, Houston
2. Heuer JK, Stubbins JF (1999) Corros Sci 41:1231
3. Nordsveen M, Nesic S, Nyborg R, Strangeland A (2003) Corrosion 59:443
4. Nesic S, Postlethwaite J, Olsen S (1996) Corrosion 52:280
5. Nesic S (2007) Corros Sci 49:4308
6. Okafor PC, Nesic S (2007) Chem Eng Comm 194:141
7. Okafor PC, Brown B, Nesic S (2009) J Appl Electrochem 39:873
8. Webster S, Harrop D, McMahon A, Partidge GJ (1993) Proceedings of NACE corrosion/1993 Paper no 109. NACE International, Houston
9. Tan YJ, Bailey S, Kinsella B (1996) Corros Sci 38:1545
10. Ramachandran S, Jovancicevic V (1999) Corrosion 55:259
11. Durnie W, Kinsella B, De Marco R, Jefferson A (2001) J Appl Electrochem 31:1221
12. Hong T, Sun YH, Jepson WP (2002) Corros Sci 44:101
13. Bilkova K, Hackerman N (2002) Proceedings of corrosion/2002 Paper no 284. NACE International, Houston
14. Lopez DA, Schreiner WH, de Sanchez SR, Simison SN (2003) Appl Surf Sci 207:69
15. Zhang G, Chena C, Lub M, Chai C, Wu Y (2007) Mater Chem Phys 105:331
16. Okafor PC, Liu X, Zheng YG (2009) Corros Sci 51(4):761
17. Liu X, Zheng YG, Okafor PC (2009) Mater & Corros 60(7):507
18. Sastri VS (1998) Corrosion inhibitors—principles and applications. Wiley, Chichester
19. Cavallro L, Bolognesi G (1946–1947) Att Acad Sci Farrara 24:1
20. Makrides AC, Hackerman N (1955) Ind Engng Chem 47:1773
21. Pillai KC, Narayan R (1978) J Electrochem Soc 125:1393
22. Ateya BG, El-Anadouli BE, El-Nizamy FM (1984) Corros Sci 24:497
23. Mendez S, Andreasen G, Schilardi PL, Figueroa M, Vazquez L, Salvarezza RS, Arvia AJ (1998) Langmuir 14:2515
24. Zhao J, Li N, Gao S, Cui G (2007) Electrochem Comm 9:2261
25. Awad MK (2004) J Electroanal Chem 567:219
26. Bonne MJ, Helton M, Edler K, Marken F (2007) Electrochem Comm 9:42
27. He XY, Deng HY, Li R, Fei XD, Wang HY, Deng ZY (2008) Acta Metall Sin (Engl Lett) 21:65
28. Wang S, Lin J, Chen F, Hu M, Hu X, Han Y, Gao Q (2004) Sci China Ser B Chem 47:480
29. Ebenso EE, Ekpe UJ, Ita BI, Offiong OE, Ibok UJ (1999) Mater Chem Phys 60:79
30. Schweinsgberg D, George G, Nanayakkawa A, Steinert D (1988) Corros Sci 28:33
31. El-Awady AA, Abd-El-Nabey BA, Aziz SG (1992) J Electrochem Soc 139:2149
32. Jutner K (1990) Electrochim Acta 35:1501
33. Paskossy T (1994) J Electrochem Soc 364:111
34. Jargelius-Pettersson RFA, Pound BG (1998) J Electrochem Soc 145:1462
35. Bai L, Conway BE (1991) J Electrochem Soc 128:2897
36. Franceschetti DR, Macdonald JR (1977) J Electrochem Soc 82:271
37. Juttner K (1990) Electrochim Acta 35:1501
38. Khaled KF, Hackerman N (2003) Electrochim Acta 48:2715
39. Khaled KF (2003) Electrochim Acta 48:2493
40. Jeyaprabha C, Sathiyanarayanan S, Venkatachari G (2006) Electrochim Acta 51:4080
41. Larabi L, Harek Y, Benali O, Ghalem S (2005) Prog Org Coat 54
42. Popova A, Sokolova E, Raicheva S, Christov M (2003) Corros Sci 45:33
43. Villamizar W, Casales M, Gonzales-Rodriguez JG, Martinez L (2006) Mater & Corros 57:696
44. Hsu CH, Manfeld F (2001) Corrosion 57:747
45. Okafor PC, Oguzie EE, Iniama GE, Ikpi ME, Ekpe UJ (2008) Glob J Pure & Appl Sci 14:89
46. Ameer MA, Khamis E, Al-Senani G (2000) Ads Sci Tech 18:177
47. Bockris JO, Swinkels DAJ (1964) J Electrochem Soc 11:736
48. Ateya BG, El-Anadouli BE, El-Nizamy FM (1984) Corros Sci 24:509
49. Durnie W, De Marco R, Jefferson R, Kinsella B (1999) J Electrochem Soc 146:1751
50. Ebenso EE, Okafor PC, Offiong OE, Ita BI, Ibok UJ, Ekpe UJ (2003) Bull Electrochem 17:459
51. Brown GM, Hope GA, Schweinsberg DP, Fredericks PM (1995) J Electroanal Chem 380:161
52. Tian M, Pell WG, Conway BE (2003) J Electroanal Chem 552:279
53. El-Egama SS (2008) Corros Sci 50:928
54. Heusler KE, Cartledge GH (1961) J Electrochem Soc 108:732
55. Kuo HC, Nobe KJ (1978) Electrochem Soc 125:853
56. MacFarlane DR, Smedley SI (1986) J Electrochem Soc 133:2240
57. Bartos M, Hackerman N (1992) J Electrochem Soc 139:2604
58. Feng Y, Siow KS, Teo WK, Hsieh AK (1999) Corros Sci 41:829
59. Okafor PC, Zheng YG (2009) Corros Sci 51:850
60. Fragnani A, Trabanelli G (1999) Corrosion 55:653
61. Oguzie EE, Li Y, Wang FH (2007) J Coll Interf Sci 310:90
62. Kuznetsov YI, Andreev NN (1996) Proceedings of corrosion/1996 paper no 214. NACE International, Houston